Eur. Phys. J. D **40**, 175–179 (2006)
DOI: 10.1140/epjd/e2006-00151-x

THE EUROPEAN PHYSICAL JOURNAL D

Three-body muon-transfer collisions from hydrogen isotope to He^{2+} and Li^{3+} ions

A. Igarashi[1,a] and N. Toshima[2]

[1] Faculty of Engineering, Miyazaki University, Miyazaki 889-2192, Japan
[2] Institute of Material Science, University of Tsukuba, Tsukuba 305-8573, Japan

Received 20 March 2006 / Received in final form 17 May 2006
Published online 28 June 2006 –

Abstract. The muon transfer rates from hydrogen isotopes (p, d) to $^{3,4}He^{2+}$ and $^{6,7}Li^{3+}$ ions are calculated in the hyperspherical close coupling method. Well converged results are obtained. The present rates are comparable to those of existing calculations for He^{2+}, but they are much larger for Li^{3+}. The resonance parameters are also calculated for resonances near the $(H\mu)_{1s}$ threshold.

PACS. 36.10.Dr Positronium, muonium, muonic atoms and molecules

1 Introduction

The transfer process of negative muons (μ) from hydrogen isotopes (H = p, or d) to helium nucleus is important in the muon catalyzed fusion [1,2]. Helium nuclei are produced by the fusion process and the helium atoms act as a muon scavenger by direct muon capture in the fusion or by the muon transfer to helium. The muon transfer from the muonic hydrogen to heavier elements is also important. When a small amount of the heavier element is added to pure hydrogen target, it may strongly influence the process of the muon catalyzed fusion [3–5].

There are two models for the muon transfer mechanism to elements of $Z > 2$ [2,6,7,9], involving the direct transfer

$$H\mu + Z \rightarrow Z\mu + H, \tag{1}$$

and the molecular transfer

$$H\mu + Z \rightarrow H\mu Z \rightarrow Z\mu + H \tag{2}$$

where a metastable $H\mu Z$ molecule is formed as an intermediate state and its decay leads to the muon transfer. The process (2) is much faster than that of (1) for the case of He [2,6] and the process (1) is expected to be more important for elements with higher Z [2]. The rates for the process (1) have been calculated as Coulomb three-body problems by neglecting atomic electrons completely. The aim of the present work is to calculate reliable muon-transfer rates for the collisions $^{3,4}He^{2+} + (H\mu)_{1s}$ and $^{6,7}Li^{3+} + (H\mu)_{1s}$ systems using the hyperspherical close coupling (HSCC) method. The studies of such collisions have many interest as examples of rearrangement scatterings with Coulomb interaction in the final states [4].

[a] e-mail: igarashi@phys.miyazaki-u.ac.jp

Muon atomic units (m.a.u), where muon mass is set to unity in addition to $\hbar = e = 1$, are used throughout this paper unless otherwise stated.

2 The HSCC method

The HSCC method is a powerful tool to study bound states and scattering states for three-body systems [11]. The present HSCC method is described in some details in [12,13]. The internal motion of three particles is described by hyperradius ρ and five angular variable Ω in the hyperspherical coordinates. The total Hamiltonian of the system is written in terms of ρ and Ω as

$$H = -\frac{1}{2M}\left(\frac{d^2}{d\rho^2} + \frac{5}{\rho}\frac{d}{d\rho}\right) + h_{ad}(\rho, \Omega), \tag{3}$$

with

$$h_{ad}(\rho, \Omega) = \frac{\Lambda^2(\Omega)}{2M} + V(\rho, \Omega) \tag{4}$$

where $\Lambda(\Omega)$ is the five-dimensional grand angular momentum operator, V is the sum of Coulomb interactions among three particles, and M is an arbitrary parameter with dimension of mass, which is taken to be reduced mass of heavy nuclei here.

The adiabatic channel functions $\{\varphi(\rho, \Omega)\}$ and the adiabatic potential $U_i(\rho)$ are defined by the eigen-value equation

$$h_{ad}(\rho, \Omega)\varphi_i(\rho, \Omega) = \left(U_i(\rho) - \frac{15}{8M\rho^2}\right)\varphi_i(\rho, \Omega), \tag{5}$$

where ρ is an adiabatic parameter.

In the HSCC method, the scattering wave function is expanded by the product of radial function $F_i(\rho)$ and φ_i as

$$\Psi^{J\Pi}(\rho,\Omega)=\sum_i^N \frac{F_i(\rho)}{\rho^{5/2}}\varphi_i(\rho,\Omega) \quad (6)$$

for each partial wave J and parity Π. Inserting this expansion in the Shrödinger equation $(H-E)\Psi^{J\Pi}=0$, we have the coupled differential equations for $\{F_i\}$

$$\left(-\frac{1}{2M}\frac{d^2}{d\rho^2}+U_i(\rho)-E\right)F_i(\rho)+\sum_j W_{ij}(\rho)F_j(\rho)=0, \quad (7)$$

where E is the total energy in the center of mass system and $W_{ij}(\rho)$ represents a non-adiabatic coupling. To obtain the scattering matrix, the wave function in equation (6) is matched with the scattering boundary conditions in the Jacobi coordinates at sufficiently large ρ. Since the system has an arrangement of a charged particle and hydrogenic atom (ion) in the asymptotic region, the dipole representation [14] is appropriate as channels in the Jacobi coordinates.

3 Results

The HSCC calculations are carried out for partial waves $J = 0$–4. Two kinds of basis sets are adopted both in $^{3,4}\mathrm{He}^{2+} + (\mathrm{H}\mu)_{1s}$ and $^{6,7}\mathrm{Li}^{3+} + (\mathrm{H}\mu)_{1s}$ collisions. Their asymptotic limits of channels are as follows;

basis set A: $\mathrm{He}^{2+} + (\mathrm{H}\mu)_{n=1}$, $\mathrm{H}^+ + (\mathrm{He}\mu)^+_{n=1-3}$
basis set B: $\mathrm{He}^{2+} + (\mathrm{H}\mu)_{n=1}$, $\mathrm{H}^+ + (\mathrm{He}\mu)^+_{n=1-4}$,

for the $\mathrm{He}^{2+} + \mathrm{H}\mu$ collision, and

basis set C: $\mathrm{Li}^{3+} + (\mathrm{H}\mu)_{n=1}$, $\mathrm{H}^+ + (\mathrm{Li}\mu)^{2+}_{n=1-3}$
basis set D: $\mathrm{Li}^{3+} + (\mathrm{H}\mu)_{n=1}$, $\mathrm{H}^+ + (\mathrm{Li}\mu)^{2+}_{n=1-4}$

for the $\mathrm{Li}^{3+} + \mathrm{H}\mu$ collision.

The muon transfer rate is defined by $\lambda = N_0 v\sigma$, where $N_0 (= 4.25 \times 10^2\ /\mathrm{cm}^3)$ is the liquid-hydrogen density, v is the collision velocity, and σ is the muon-transfer cross section.

3.1 $^{3,4}\mathrm{He}^{2+} + (^{1,2}\mathrm{H}\mu)_{1s}$ collisions

The S-wave adiabatic potential curves for the $^3\mathrm{He}^{2+} + p\mu$ system are shown in Figure 1. Each potential curve converges to the atomic energy of $(p\mu)$ or $(\mathrm{He}\mu)^+$ as $\rho \to \infty$, and the corresponding adiabatic channel function describes the fragmentation into $\mathrm{He}^{2+} + (p\mu)$ or $p + (\mathrm{He}\mu)^+$. The potential curve corresponding to the initial channel, $\mathrm{He}^{2+} + (p\mu)_{n=1}$, is close to those leading to $p + (\mathrm{He}\mu)^+_{n=2}$. The coupling of $(\mathrm{He}\mu)^+_{n=2}$ channels with $(p\mu)_{n=1}$ channel is considerable for $\rho < 15$. However, the transfer to $(\mathrm{He}\mu)^+_{n=2}$ channels is less probable at low energies owing to the Coulomb repulsion between H^+ and He^+. Thus, the muon transfer to the low-lying $(\mathrm{He}\mu)^+_{n=1}$ state is dominant at low energies.

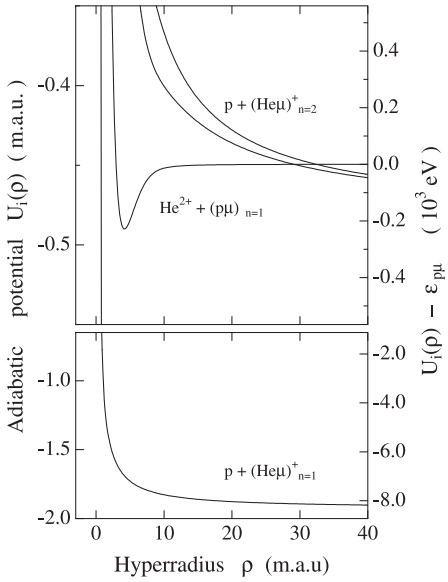

Fig. 1. The S wave adiabatic potential curves of $^3\mathrm{He}^{2+} + p\mu$ system. The asymptotic fragmentation described by corresponding adiabatic channel function is indicated as $p + (\mathrm{He}\mu)^+_n$ or $\mathrm{He}^{2+} + (p\mu)_n$. The notation $\epsilon_{p\mu}$ denotes the atomic energy of $(p\mu)_{1s}$.

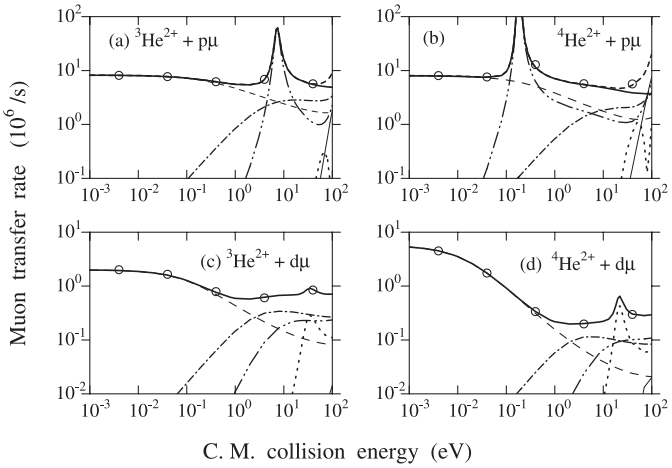

Fig. 2. The muon transfer rates for the $\mathrm{He}^{2+} + (\mathrm{H}\mu)_{1s}$ collisions. Partial wave rate calculated with basis set B: $J = 0$ (dashed curve), $J = 1$ (dot-dashed curve), $J = 2$ (dot-dot-dashed curve), $J = 3$ (dotted curve), $J = 4$ (solid curve). Summed rate for $J = 0$–4: transfer to $(\mathrm{He}\mu)^+_{n=1}$ calculated with basis set B (bold solid curve), transfer to $(\mathrm{He}\mu)^+_{n=1,2}$ calculated with basis set B (bold dashed curve), transfer to $(\mathrm{He}\mu)^+_{n=1,2}$ calculated with basis set A (circles). The transfer rate to $n = 2$ states is negligibly small in the $^{3,4}\mathrm{He}^{2+} + (d\mu)_{1s}$ collisions in the figure.

The sum of muon-transfer rates up to $J = 4$ and their partial-wave contributions are depicted in Figure 2 for the center-of-mass collision energy $0.001 \le E_c \le 100$ in eV. The calculations using basis sets A and B give similar results, and the convergence is good with respect to the

Table 1. Comparison of muon transfer rate (10^6/s) in the $He^{2+} + (H\mu)_{1s}$ collision at center-of-mass collision energy E_c.

	$^3He^{2+}$	$^4He^{2+}$	$^3He^{2+}$	$^4He^{2+}$
E_c (eV)	$p\mu$		$d\mu$	
0.001	8.18^a	8.04^a	1.98^a	5.30^a
0.004	8.13^a	7.98^a	1.94^a	4.52^a
	110	59	258	552
0.01	8.04^a	7.86^a	1.87^a	3.52^a
0.04	7.70^a	7.54^a	1.60^a	1.74^a
	91^b	48^b	162^b	218^b
	6.3^c	5.5^c	1.3^c	1.0^c
	17^d	17^d	17^d	17^d
	8.4^e	6.8^e	5.2^e	5.0^e
0.1	7.25^a	9.60^a	1.27^a	0.92^a
	82^b	42^b	126^b	134^b
	8.3^e		5.1^e	
0.4	6.19^a	11.6^a	0.76^a	0.34^a
1.0	5.56^a	7.11^a	0.59^a	0.22^a
	8.1^e		4.7^e	
4.0	6.84^a	5.53^a	0.62^a	0.20^a
10.0	16.0^a	4.96^a	0.68^a	0.22^a

[a] Present calculation with basis set A. [b] Molecular transfer rate of Kravtsov et al. [6]. [c] Matveenko and Ponomarev [1]. [d] Radiative transfer rate of Czaplinski et al. [10]. [e] Sultanov and Adhikari [4].

basis set. S-wave is dominant for low collision energy and the contribution from higher partial waves become large with increasing energy. The muon transfer of $(He\mu)_{n=2}$ becomes important for $E_c > 10$ eV in $p\mu$ target. Though it is negligible for $E_c \leq 100$ eV in $d\mu$ target, it comes to contribute for $E_c \gg 100$ eV.

The obtained muon transfer rates are compared in Table 1 with those of other works involving the perturbed stationary state (PSS) calculation [1] and the Faddeev-Hahn-type calculation [4], in which the muon transfer rates are calculated in the direct muon transfer model (1). The rates in the PSS calculation are fairly close to the present ones at $E_c = 0.04$ eV, but the agreement with the Faddeev-Hahn-type calculation is rather poor. The disagreement is worse for the $d\mu$ target than for the $p\mu$ target. Table 1 also includes the molecular [6] and the radiative [10] transfer rates, which are much larger than that of direct transfer.

The D-wave contributions of Figures 2a and 2b show resonance structures. Figures 3a and 3b, respectively, give the rate in the resonance region and the adiabatic potentials of the initial channel for the $^4He^{2+} + (p\mu)_{1s}$ collision. It is well seen from Figure 3b that the adiabatic potentials of the $^4He^{2+}+(p\mu)_{1s}$ channel support Feshbach resonances in $J = 0$ and 1 and a shape resonance in $J = 2$. For D-wave resonance in the $^4He^{2+} + p\mu$ system, the resonance energy and width are $E_c = 0.18$ eV and 7×10^{-4} eV, respectively, with the basis set B. The resonance parameter is derived by fitting the eigen phase sum to the Breit-Wigner formula with a linear background. Resonances near the $(H\mu)_{1s}$ threshold in the $^{3,4}He^{2+} + ^{1,2}H\mu$ systems are summarized in Table 2, where the results of Belyaev et al. [15] and Kravosov and Mikhailov [16] are included for comparison. The calculations for resonances below the $(H\mu)_{n=1}$ threshold are treated in several works, which are given in [15,16]. The present results are consistent with those of [15,16].

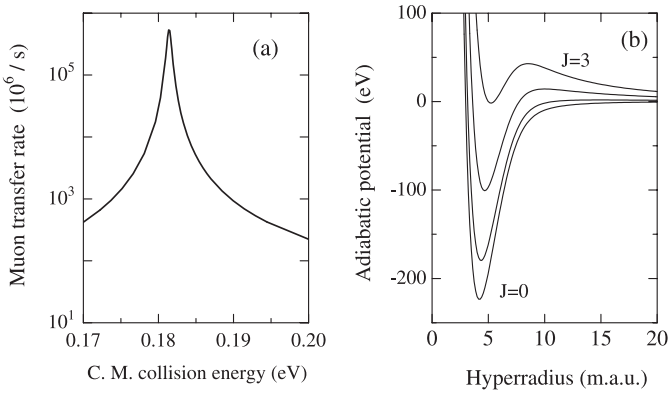

Fig. 3. (a) The muon transfer rate for energies near the D-wave resonance in the $^4He^{2+} + (p\mu)_{1s}$ collision. (b) The adiabatic potential curves converging to the energy of $(p\mu)_{1s}$ for the $^4He^{2+} + p\mu$ system. The potential curves are for $J = 0$–3 from the bottom.

Table 2. Resonances associated with $(H\mu)_{1s}$ threshold of the $He^{2+} + H\mu$ system. Each resonance is expressed as (E_r, Γ) in eV, where E_r is the resonance energy measured from the $(H\mu)_{1s}$ threshold and Γ is the width. $x[y] = x \times 10^y$.

Partial wave	$^3He^{2+} + p\mu$	$^4He^{2+} + p\mu$
$J = 0$	$(-73.70, 5.6[-3])^a$	$(-81.69, 3.9[-3])^a$
	$(-72.76, 6.4[-3])^b$	$(-80.64, 4.7[-3])^b$
	$(-73.2, \text{——})^c$	$(-80.8, \text{——})^c$
$J = 1$	$(-41.73, 2.8[-3])^a$	$(-50.51, 2.2[-3])^a$
	$(-38.82, 3.1[-3])^b$	$(-47.45, 2.5[-3])^b$
	$(-41.5, \text{——})^c$	$(-50.0, \text{——})^c$
$J = 2$	$(7.2, 1.9)^a$	$(0.205, 7.9[-4])^a$
	$(7.2, 1.9)^d$	$(0.181, 6.7[-4])^d$
	$^3He^{2+} + d\mu$	$^4He^{2+} + d\mu$
$J = 0$	$(-70.90, 3.5[-4])^a$	$(-79.36, 9.9[-5])^a$
	$(-69.37, 1.9[-4])^b$	$(-77.49, 4.8[-5])^b$
	$(-71.0, \text{——})^c$	$(-79.4, \text{——})^c$
$J = 1$	$(-48.33, 3.8[-4])^a$	$(-58.14, 1.3[-4])^a$
	$(-46.31, 2.1[-4])^b$	$(-55.74, 7.9[-5])^b$
	$(-48.5, \text{——})^c$	$(-58.3, \text{——})^c$
$J = 2$	$(-9.46, 1.7[-4])^a$	$(-20.48, 9.5[-5])^a$
	$(-7.11, 1.2[-4])^b$	$(-17.49, 6.9[-5])^b$
$J = 3$	$(30.4, 20)^a$	$(20.5, 8.1)^a$
	$(30.0, 20)^d$	$(20.3, 7.8)^d$

[a] Present calculation with basis set A. [b] Belyaev et al. [15]. [c] Kravtsov and Mikhailov [16]. [d] Present calculation with basis set B.

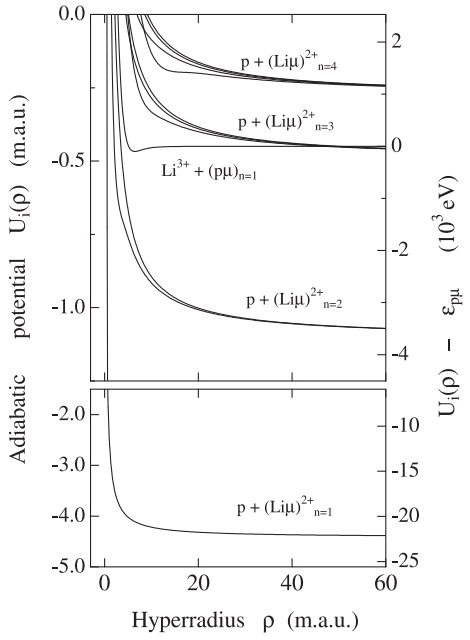

Fig. 4. The S wave adiabatic potential curves of $^6\mathrm{Li}^{3+}+p\mu$ system. The asymptotic fragmentation described by corresponding adiabatic channel function is indicated as $p+(\mathrm{Li}\mu)^{2+}_n$ or $\mathrm{Li}^{3+}+(p\mu)_n$. The notation $\epsilon_{p\mu}$ denotes the atomic energy of $(p\mu)_{1s}$.

3.2 $^{6,7}\mathrm{Li}^{3+}+(^{1,2}\mathrm{H}\mu)_{1s}$ collisions

The S-wave adiabatic potential curves for the $^6\mathrm{Li}^{3+}+p\mu$ system are shown in Figure 4 as an example of $\mathrm{Li}^{3+}+\mathrm{H}\mu$ systems. The muon transfer into $(\mathrm{Li}\mu)_{n=2}$ is predominant at low energy collisions. The potential curves which describe fragmentation $p+(\mathrm{Li}\mu)^{2+}_{n=3}$ are repulsive, and the muon transfer into $(\mathrm{Li}\mu)_{n=3}$ is suppressed at low energies. The contributions of transfer to states with $n=1$ and $n=3$ are negligible for $E_c\le 100$ eV, but the transition to the $n=3$ states is expected to be important for higher energies.

The muon transfer rates for the $^{6,7}\mathrm{Li}^{3+}+(^{1,2}\mathrm{H}\mu)_{1s}$ collisions are shown in Figure 5. The rates obtained with the two basis sets C and D agree well, which shows good convergence with respect to basis sets. It seems better to include higher partial-wave contribution for $E_c>10$ eV for $d\mu$ target.

The energy dependence of muon transfer rate is more similar for $^{6,7}\mathrm{Li}^{3+}$ than for $^{3,4}\mathrm{He}^{2+}$ in $p\mu$ target or $d\mu$ target, since the reduced mass of system is closer to the mass of $p\mu$ or $d\mu$ for heavier ion. Peak structures are seen for $J=2$ in $p\mu$ target (Figs. 4a, 4b) and for $J=3$ in $d\mu$ target (Figs. 4c, 4d). The peak widths are comparable to the collision energy.

The rates for muon transfer are tabulated in Table 3, which includes the results of the Faddeev-Hahn-type calculation by Sultanov and Adhikari [4] and the molecular muon transfer rates calculated by Ivanov et al. [8]. The present rates are much larger than those of the Faddeev-Hahn-type calculation and those of the molecular transformation, indicating that the direct muon transfer is important in the muon transfer to Li.

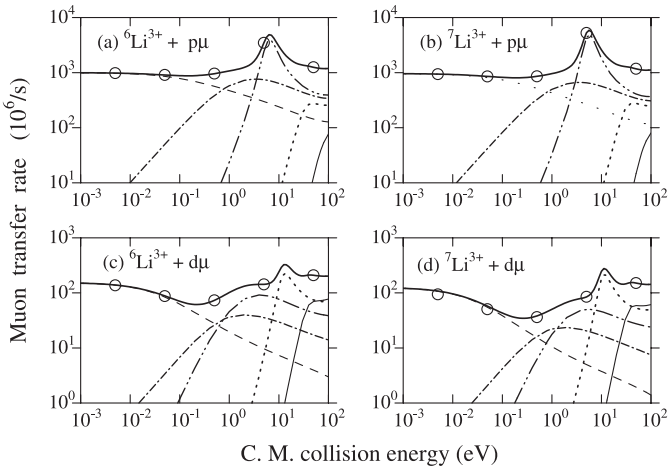

Fig. 5. The muon transfer rates for the $\mathrm{Li}^{3+}+(\mathrm{H}\mu)_{1s}$ collisions. Partial wave rate calculated with basis set D: $J=0$ (dashed curve), $J=1$ (dot-dashed curve), $J=2$ (dot-dot-dashed curve), $J=3$ (dotted curve), $J=4$ (solid curve). Summed rate for $J=0$–4: basis set C (circle), basis set D (bold solid curve).

Table 3. Comparison of muon transfer rate (10^8/s) for the $\mathrm{Li}^{3+}+(\mathrm{H}\mu)_{1s}$ collisions at center-of-mass collision energy E_c. $x[y]=x^y$.

	$^6\mathrm{Li}^{2+}$	$^7\mathrm{Li}^{2+}$	$^6\mathrm{Li}^{3+}$	$^7\mathrm{Li}^{3+}$
E_c (eV)	$p\mu$		$d\mu$	
0.001	9.95[a]	9.57[a]	1.50[a]	1.21[a]
0.004	9.84[a]	9.45[a]	1.42[a]	1.11[a]
	5.0[−3][c]	3.8[−3][c]	2.78[−2][c]	3.17[−2][c]
0.01	9.67[a]	9.25[a]	1.28[a]	0.96[a]
0.04	9.15[a]	8.67[a]	0.95[a]	0.63[a]
			1.9[−2][b]	1.6[−2][b]
	3.8[−3][c]	2.8[−3][c]	9.1[−3][c]	8.2[−3][c]
0.1	8.82[a]	8.21[a]	0.71[a]	0.43[a]
			1.9[−2][b]	1.6[−2][b]
	3.1[−3][c]	2.3[−3][c]	5.6[−3][c]	4.7[−3][c]
0.4	9.30[a]	8.35[a]	0.68	0.36[a]
1.0	10.7[a]	9.59[a]	1.02[a]	0.50[a]
			1.2[−2][b]	1.2[−2][b]
	1.6[−3][c]	1.2[−3][c]	1.6[−3][c]	1.2[−3]
4.0	22.1[a]	30.3[a]	1.43[a]	0.80[a]
10.0	30.1[a]	25.8[a]	2.41[a]	2.46[a]

[a] Present calculation with basis set B. [b] Sultanov and Adhikari [4]. [c] Molecular muon transfer rate of Ivanov et al. [8].

The potential curves for the $\mathrm{Li}^{3+}+(\mathrm{H}\mu)_{1s}$ channel support resonances for low partial waves. The resonance parameters are tabulated in Table 4. The present calculation gives deeper resonance energies than the calculation of Kravtsov et al. [17]. The widths are broader for Li ions than those of He ions. The larger width is consistent with larger cross-section for Li than that for He, since the

Table 4. Resonances associated with $(H\mu)_{1s}$ threshold of the $Li^{3+}+H\mu$ system. Each resonance is expressed as (E_r, Γ) in eV, where E_r is the resonance energy measured from the $(H\mu)_{1s}$ threshold and Γ is the width. $x[y] = x \times 10^y$.

Partial wave	$^6Li^{3+} + p\mu$	$^7Li^{3+} + p\mu$
$J = 0$	$(-18.4, 0.25)^a$	$(-19.3, 0.23)^a$
	$(-17.6, —)^b$	$(-18.5, —)^b$
$J = 1$	$(-8.4, 0.17)^a$	$(-9.3, 0.16)^a$
	$(-6.96, —)^b$	$(-7.9, —)^b$
$J = 2$	$(5.78, 4.6)^a$	$(5.15, 3.6)^a$
	$^6Li^{3+} + d\mu$	$^7Li^{3+} + d\mu$
$J = 0$	$(-20.25, 1.4[-2])^a$	$(-21.40, 6.7[-3])^a$
	$(-19.8, —)^b$	$(-21.0, —)^b$
$J = 1$	$(-13.52, 1.7[-2])^a$	$(-14.76, 1.0[-2])^a$
	$(-12.9, —)^b$	$(-14.1, —)^b$
$J = 2$	$(-1.62, 1.5[-2])^a$	$(-2.87, 1.2[-2])^a$
	$(-0.84, —)^b$	$(-2.02, —)^b$
$J = 3$	$(10.0, 7.0)^a$	$(9.98, 7.0)^a$

[a] Present calculation with basis set C. [b] Kravtsov et al. [17].

resonances $(H\mu Z)$ below the $(H\mu)_{1s}$ threshold mainly decay through couplings with $H^+ + (He\mu)^+_{n=1}$ channels and with $H^+ + (Li\mu)^{2+}_{n=2}$ channels for He and Li, respectively.

4 Summary

The HSCC method is applied to calculate the three-body muon transfer rate in the $He^{2+}+(H\mu)_{1s}$ and $Li^{3+}+(H\mu)_{1s}$ collisions, and electrons in He and Li are completely neglected. The present calculation shows good convergence with respect to the basis sets, and it seems to be reliable.

The transfer to $(He\mu)^+_{n=1}$ is dominant at lower energies in the He^{2+} collision. The present transfer rate is within the same order as those calculated in the three body treatments [1,4,9]. The molecular transfer [6] is roughly 10 times faster than the direct transfer in the $He + p\mu$ system and 100 times in the $He + d\mu$ system.

For the case of Li^{3+} impact, $(Li\mu)^{2+}$ is formed in the $n = 2$ states for $E_c \leq 100$ eV. The present direct transfer rates are about 50 times as large as those calculated with the Faddeev-Hahn-type calculation [4] and are three orders of magnitude larger than the molecular transfer rates [7].

References

1. A.V. Matveenko, L.I. Ponomarev, Sov. Phys. JETP **36**, 24 (1973)
2. S. Tresch et al., Phys. Rev. A **57**, 2496 (1998)
3. H.E. Rafelski, D. Harley, G.R. Shin, J. Rafelski, J. Phys. B **24**, 1469 (1991)
4. R.A. Sultanov, S.K. Adhikari, J. Phys. B **32**, 5751 (1999)
5. R.A. Sultanov, S.K. Adhikari, Phys. Rev. A **62**, 22509 (2000) and references therein
6. A.V. Kravtsov, A.I. Mikhailov, N.P. Popov, J. Phys. B **19**, 2579 (1986)
7. A.V. Kravtsov, A.I. Mikhailov, N.P. Popov, J. Phys. B **19**, 1323 (1986)
8. V.K. Ivanov, A.V. Kravtosov, A.I. Mikhailov, N.P. Popov, Z. Phys. D **7**, 349 (1988)
9. W. Czapliński, A.I. Mikhailov, Phys. Lett. A **169**, 181 (1992)
10. W. Czapliński, A.I. Mikhailov, I.A. Mikhailov, Hyperfine Int. **142**, 577 (2002)
11. C.D. Lin, Phys. Rep. **257**, 1 (1995)
12. A. Igarashi, N. Toshima, T. Shirai, Phys. Rev. A **50**, 4951 (1994)
13. A. Igarashi, I. Shimamura, N. Toshima, New J. Phys. **2**, 17 (2000)
14. M. Gailitis, R. Damburg, Proc. Phys. Soc. **82**, 192 (1963)
15. V.B. Belyaev et al., Z. Phys. D **41**, 239 (1997)
16. A.V. Kravtsov, A.I. Mikhailov, JETP **90**, 45 (2000)
17. A.V. Kravtsov, N.P. Popov, G.E. Solyakin, Sov. J. Nucl. Phys. **35**, 876 (1982)